



タイトル Title	Unusual magnetic and superconducting characteristics in multilayered high-Tc cuprates: 63Cu NMR study
著者 Author(s)	Kotegawa, Hisashi / Tokunaga, Y / Ishida, K / Zheng, G.-q / Kitaoka, Y / Kito, H / Iyo, A / Tokiwa, K / Watanabe, T / Ihara, H
掲載誌・巻号・ページ Citation	Physical Review B,64:064515
刊行日 Issue date	2001-08
資源タイプ Resource Type	Journal Article / 学術雑誌論文
版区分 Resource Version	publisher
権利 Rights	
DOI	10.1103/PhysRevB.64.064515
JaLCDDOI	
URL	http://www.lib.kobe-u.ac.jp/handle_kernel/90002677

Unusual magnetic and superconducting characteristics in multilayered high- T_c cuprates: ^{63}Cu NMR study

H. Kotegawa,^{1,*} Y. Tokunaga,^{1,*} K. Ishida,^{1,*} G.-q. Zheng,¹ Y. Kitaoka,^{1,*} H. Kito,^{2,*} A. Iyo,^{2,*} K. Tokiwa,^{3,*} T. Watanabe,^{3,*} and H. Ihara^{2,*}

¹*Department of Physical Science, Graduate School of Engineering Science, Osaka University, Toyonaka, Osaka 560-8531, Japan*

²*Electrotechnical Laboratory, Umezono, Tsukuba 305-8568, Japan*

³*Department of Applied Electronics, Science University of Tokyo, Yamazaki, Noda, Chiba 278-8510, Japan*

(Received 27 December 2000; published 23 July 2001)

We report unusual magnetic and superconducting (SC) characteristics in multilayered CuO_2 planes in Hg- and Cu-based high- T_c cuprates through the ^{63}Cu -NMR measurements. These compounds, in which the number of CuO_2 planes (n) ranges from 3 to 5 in a unit cell, include crystallographically inequivalent outer (OP) and inner (IP) CuO_2 plane that are surrounded by pyramidal and square oxygen, respectively. The Knight shift (^{63}K) at the OP and IP exhibits respective characteristic temperature dependence, consistent with its own doping level. Using an experimental relation between the spin part in ^{63}K at room temperature and the doping level in a CuO_2 layer N_h , we show that $N_h(\text{OP})$ at the OP is larger than $N_h(\text{IP})$ at the IP for all the systems and its difference $\Delta N_h = N_h(\text{OP}) - N_h(\text{IP})$ increases as either a total carrier content δ or n increases. At ΔN_h 's exceeding a critical value, the pseudogap behavior in the normal state is seen alone at the IP, and a bulk SC transition does not set in simultaneously at the IP and OP. A SC nature at the OP becomes consistent with a mean-field behavior only below T_{c2} that is significantly lower than T_c . Reduction in T_c with increasing n is associated with an increase in ΔN_h . It is a rather remarkable aspect that a T_c is not always reduced even though these multilayered high- T_c compounds are heavily overdoped. This arises, we show, because the IP remains underdoped and keeps a high value of T_c , while the OP is predominantly overdoped. This may be a microscopic origin for the lowest anisotropic SC characteristics reported to date in Cu-based multilayered high- T_c compounds.

DOI: 10.1103/PhysRevB.64.064515

PACS number(s): 76.60.Cq, 76.60.Es, 71.27.+a, 75.20.Hr

I. INTRODUCTION

Extensive investigations have recently been made on various multilayered high- T_c cuprates that include three or more CuO_2 layers in a unit cell. Their superconducting (SC) characteristics have been reported to depend closely on the doping level in the CuO_2 layer N_h and on the number of CuO_2 planes n per unit cell. In most of high- T_c compounds, T_c varies as a bell-shaped curve with N_h and exhibits a maximum value $T_{c,max}$ at $N_h(\text{optimum}) \sim 0.2$. In $(\text{Cu,C})\text{Ba}_2\text{Ca}_3\text{Cu}_4\text{O}_{10+y}$ ($n=4$ Cu1234), however, $T_c = 117$ K was reported to be almost independent of the doping level even though in the heavily overdoped region.¹ This feature is believed to lead to the lowest anisotropic SC characteristics reported to date that is promising for an application use.² It is an unsettled issue why a $T_{c,max}$ increases monotonically with increasing n , but saturates at either $n = 3$ or 4 ,³ which is suggested to be the optimum number of n that maximizes T_c . A cause for the suppression in $T_{c,max}$ for $n \geq 4$ is not fully understood yet.

In mono-layered or bi-layered compounds, N_h is uniform at the crystallographically equivalent CuO_2 planes. This is, however, not the case in multilayered compounds for $n \geq 3$ in which there exist crystallographically inequivalent outer (OP) and inner (IP) CuO_2 planes. The former and latter are characterized by a pyramidal (five) and a square (four) oxygen coordination, respectively. Extensive NMR studies suggested that respective local doping levels $N_h(\text{OP})$ and $N_h(\text{IP})$ differ at the IP and OP. Their T variations of $1/T_1T$

and Knight shift were confirmed to be the same.⁴⁻¹⁰ On the other hand, as a difference $\Delta N_h = N_h(\text{OP}) - N_h(\text{IP})$ becomes larger, disparate SC and magnetic behaviors were reported at the OP and IP for an overdoped Cu1234 ($n=4$).¹¹ Namely, the normal-state magnetic behaviors for the IP and OP are characteristic of underdoped and overdoped compounds, respectively. An SC gap fully develops at the IP below $T_c = 117$ K, but it increases gradually and linearly at the OP down to $T_{c2} = 60$ K. Thus, it was recognized that the SC and magnetic properties in multilayered compounds are intimately affected by a possible variation in $N_h(\text{IP})$ and $N_h(\text{OP})$ as well as by a total doping level per unit cell δ .

In this paper, we report extensive ^{63}Cu -Knight shift ^{63}K measurements on two series of multilayered compounds, $\text{HgBa}_2\text{Ca}_{n-1}\text{Cu}_n\text{O}_{2n+2+y}$ and $\text{CuBa}_2\text{Ca}_{n-1}\text{Cu}_n\text{O}_{2n+4-y}$ with $n = 3, 4$ and 5 and different hole content δ . The ^{63}K at the IP and OP exhibits respective characteristic temperature dependence, consistent with its own doping level. Local doping levels $N_h(\text{IP})$ and $N_h(\text{OP})$ at the IP and OP are separately extracted from the spin part in ^{63}Cu -Knight shift, $K_s(\text{RT})$ at room temperature (RT). We remark that the highest $T_c = 133$ K to date in Hg1223 ($n=3$) is because both the OP and IP are nearly optimally doped. $N_h(\text{OP})$ is shown to increase predominantly, whereas $N_h(\text{IP})$ remains in an underdoped region, when either n or δ increases. As a difference $\Delta N_h = N_h(\text{OP}) - N_h(\text{IP})$ increases, disparate magnetic and SC behaviors are found at the IP and OP such that the pseudogap behavior is seen alone at the IP, and a bulk SC transition does not set in simultaneously at the IP and OP.

TABLE I. Listed are for various multilayered high- T_c compounds the superconducting transition temperature T_c , the pseudogap temperature T^* below which the $1/T_1T$ decreases, respective local doping levels $N_h(\text{IP})$ and $N_h(\text{OP})$ at the inner and outer CuO_2 plane that were extracted from the ^{63}Cu Knight-shift measurement, a total doping level in a unit cell $\delta = (n-2)N_h(\text{IP}) + nN_h(\text{OP})$ where n is the number of CuO_2 planes, a difference in doping level $\Delta N_h = N_h(\text{OP}) - N_h(\text{IP})$, $t_c(\text{K})$ and $t^*(\text{K})$ that is defined as respective characteristic temperatures where $d(K_{s,ab})/dT$ have a distinct peak and begins to deviate steeply from a linear T variation with decreasing T . Note that t^* is almost the same as T^* , $t_c(\text{IP})$ is the same as T_c , but $t_c(\text{OP})$ is lower than T_c when $\sim 0.07 < \Delta N_h$ (see the text).

$n(n_{\text{IP}} + n_{\text{OP}})$	3(1+2)				4(2+2)			5(3+2)
	Hg1223 (a)	Cu1223 (b)	Hg1223 (c)	Cu1223 (d)	Hg1234 (e)	Cu1234 (f)	Cu1234 (g)	Cu1245 (h)
T_c (K)	115	119	133	71	123	106	117	90
T^* (K)	230	140	160	70	180	140	150	160
$N_h(\text{IP})$	0.189	0.192	0.207	0.217	0.158	0.168	0.192	0.169
$N_h(\text{OP})$	0.196	0.230	0.252	0.290	0.218	0.247	0.313	0.277
δ	0.574	0.653	0.712	0.797	0.752	0.829	1.01	1.06
ΔN_h	0.014	0.039	0.045	0.073	0.060	0.079	0.121	0.108
t_c (K) IP/OP	115	115	132	56	117	105/50	115/60	90/65
t^* (K)	285	150	160	75	210	160	160	135

The SC nature at the OP becomes consistent with a mean-field behavior only below T_{c2} that is significantly lower than T_c . It is a notable aspect that T_c is not reduced even though these multilayered high- T_c compounds are heavily overdoped.¹ We remark that this arises because the IP remains underdoped and keeps a high value of T_c , even though the OP is predominantly overdoped.

II. EXPERIMENTAL RESULTS AND DISCUSSION

All the multilayered compounds used in this study were prepared by a high-pressure synthesis technique as described elsewhere.¹² Crystal structures and lattice parameters are reported to be nearly the same in these Hg- and Cu-based compounds.^{13–15} Powder x-ray diffraction experiment confirmed that the samples consist of almost a single phase.¹² A SC transition temperature, T_c was determined at an onset temperature below which diamagnetic signal appears in dc susceptibility. The T_c of all the samples is listed in Table I. For NMR measurements, the powder samples, which were aligned along the c axis at an external magnetic field of $H = 16$ T, were fixed with the stycast 1266 epoxy. The NMR experiments were performed by the conventional spin-echo method at 174.2 MHz ($H \sim 15.3$ T) and a T range of 4.2–300 K.

Figure 1 indicates typical NMR spectra for the central transition ($1/2 \leftrightarrow -1/2$) in a series of $(\text{Cu,C})\text{Ba}_2\text{Ca}_{n-1}\text{Cu}_n\text{O}_{2n+4-y}$ with $n=3, 4$ and 5 . All the spectra consist of well separated two peaks. Since the relative intensity after T_2 correction of the sharper peak increases with increasing IP layers, the sharper low-field peak and the broader high-field peak are assigned to come from the IP and OP, respectively. This assignment is consistent with the previously reported three-layer $\text{Tl}_2\text{Ba}_2\text{Ca}_2\text{Cu}_3\text{O}_{10}$ (Tl2223) where the intensity of the broader and low-field peak is exactly twice of that for the sharper and high-field

peak.⁷ The fact that the spectral width is much narrower for the IP than for the OP reveals that some disorder is smaller at the IP than at the OP. This may be because the IP is far from the charge-reservoir layer where some randomness is introduced due to doping holes.

In general, the observed Knight shift, $K(T)$ consists of a T -independent orbital part K_{orb} , and a T -dependent spin part $K_s(T)$ that is proportional to the uniform susceptibility χ_s . Taking into account that $K(T)$ is anisotropic, it is expressed

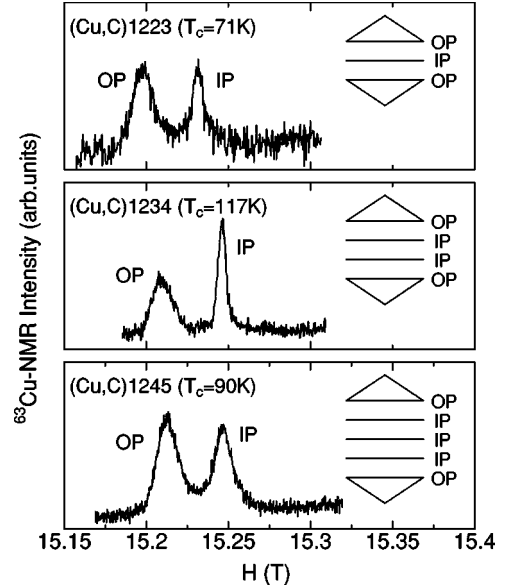


FIG. 1. ^{63}Cu -NMR spectra at $H \parallel c$ axis and $T=160$ K for $n=3$ Cu1223, $n=4$ Cu1234, and $n=5$ Cu1245. Here n is the number of CuO_2 planes. A sharp peak at a high-field side comes from the IP, whereas a broad one at a low-field side from the OP. Here the IP and OP are the inner and outer CuO_2 plane, respectively, as indicated in the inset.

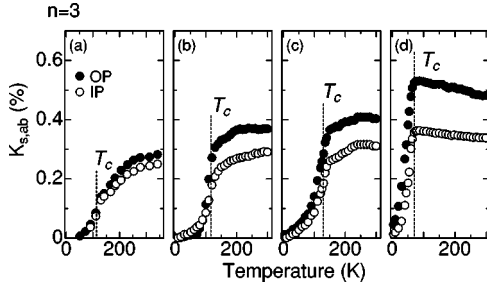


FIG. 2. The T dependence of the spin part in the ^{63}Cu Knight shift $K_{s,ab}$ at $H \parallel c$ axis for the $n=3$ compounds with various doping levels [see (a)–(d) in Table I].

as $K_\alpha(T) = K_{s,\alpha}(T) + K_{orb,\alpha}$ ($\alpha = ab$ and c). The $K_s(T)$ in underdoped compounds decreases with decreasing T due to both effects of the development of antiferromagnetic spin correlations and the opening of pseudogap. On the other hand, $K_s(T)$ in the overdoped ones is nearly T independent. It is noteworthy that $K_s(\text{RT})$ at RT increases as N_h increases in high- T_c compounds.

Figures 2(a) and 2(c) show the T dependence of $K_{s,ab}(T)$ at $H \parallel ab$ plane for $\text{HgBa}_2\text{Ca}_2\text{Cu}_3\text{O}_{8+y}$ ($n=3$ Hg1223),^{9,8} and Figs. 2(b) and 2(d) for $(\text{Cu,C})\text{Ba}_2\text{Ca}_2\text{Cu}_3\text{O}_{10-y}$ ($n=3$ Cu1223). Here all the doping levels are different. These compounds include one IP and two OP's. Respective Figs. 3(e), 3(f), and 3(g) indicate the $K_{s,ab}(T)$'s for $\text{HgBa}_2\text{Ca}_3\text{Cu}_4\text{O}_{10+y}$ ($n=4$ Hg1234), $(\text{Cu,Ni})\text{Ba}_2\text{Ca}_3\text{Cu}_4\text{O}_{12-y}$, and $(\text{Cu,C})\text{Ba}_2\text{Ca}_3\text{Cu}_4\text{O}_{12-y}$ ($n=4$ Cu1234) that include two IP's and OP's. Figure 3(h) indicates the $K_{s,ab}$ for $(\text{Cu,C})\text{Ba}_2\text{Ca}_4\text{Cu}_5\text{O}_{14-y}$ ($n=5$ Cu1245) that includes two OP's and three IP's. The respective data in Figs. 2(a) and 2(c) are cited from the paper reported by Julien *et al.*⁹ and Magishi *et al.*⁸ In all the compounds, it is evident that $K_{s,ab}(T)$ is larger for the OP than for the IP. In the $n=3$ Hg1223 [see Fig. 2(a)] and $n=4$ Hg1234 [see Fig. 3(e)], since the $K_{s,ab}(T)$'s at the OP and IP decrease with decreasing T , both the IP and OP are expected to be underdoped. By contrast, in the $n=4$ Cu1234 [see Figs. 3(f) and 3(g)] and $n=5$ Cu1245 [see Fig. 3(h)], the $K_{s,ab}$ at the IP decreases with decreasing T , whereas the $K_{s,ab}$ at the OP that is largely enhanced is nearly T independent down to T_c . This evidences that the OP is heavily overdoped, but the IP remains underdoped.

In order to see in detail the T dependence of $K_{s,ab}$ below

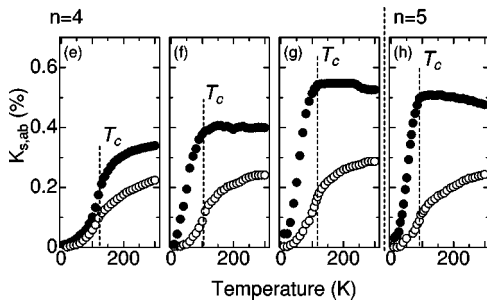


FIG. 3. The T dependence of $K_{s,ab}(T)$ for the $n=4$ and 5 compounds with various doping levels [see (e)–(h) in Table I].

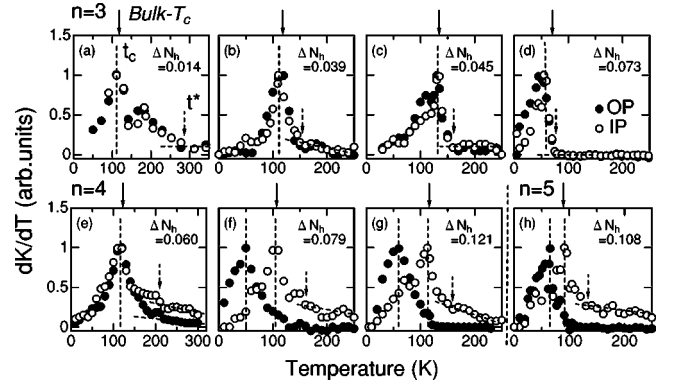


FIG. 4. The T dependence of T derivatives of $K_{s,ab}$, $dK_{s,ab}(T)/dT$ for $n=3$, 4 and 5 compounds [see (a)–(h) in Table I]. The dotted line (arrow) shows t_c (t_*). The solid arrow shows bulk T_c .

T_c from Figs. 2(a–d) and 3(e–h), its T -derivative value $d(K_{s,ab})/dT$ is plotted as a function of T in Fig. 4. As shown in the figure, t_c and t^* are defined as respective characteristic temperatures where $d(K_{s,ab})/dT$ have a distinct peak and begins to deviate steeply from a gradual T variation with decreasing T . The values of t_c and t^* for various multilayered compounds are collected in Table I. In the $n=3$ compounds [(a)–(d)] and the $n=4$ Hg1234 [(e)], t_c is the same as a bulk SC transition temperature T_c , while t^* is close to a pseudogap temperature T^* that was determined from the T dependence of $1/T_1 T$.^{8,9,11,16} In these compounds, both the t_c and t^* are almost the same at the IP and OP as expected. In the $n=4$ Cu1234 compounds [(f) and (g)] and $n=5$ Cu1245 [(h)], on the other hand, it is unconventional that t_c and t^* differ at the IP and OP. Note that the $t_c(\text{IP})$ at the IP is in accord with the bulk T_c . We remark that t^* at the overdoped OP does not always correspond to T^* , although t^* at the IP does to T^* . It is apparent that $t_c(\text{OP})$ that is denoted as T_{c2} is lower than T_c . The previous study on $n=4$ Cu1234 ($T_c = 117$ K and $T_{c2} = 60$ K) revealed that the SC gap at the OP does not fully develop down to $T_{c2} = 60$ K.¹¹ From comparison with a conventional d -wave model, it was shown that its SC gap increases gradually and linearly below T_c and follows the BCS mean-field type of T dependence below T_{c2} . These disparate SC and magnetic behaviors are considered to originate from a larger difference $\Delta N_h = N_h(\text{OP}) - N_h(\text{IP})$.

We try to estimate $N_h(\text{OP})$ and $N_h(\text{IP})$ by using an experimental relation between $K_{s,ab}(\text{RT})$ and N_h that was deduced from the nuclear quadrupole resonance (NQR) frequency, ν_Q .^{7,17} Zheng *et al.* argued that ν_Q at the planer Cu and O site are determined by the respective on-site hole density. They succeeded in evaluating each local hole content at the planer Cu and O site, $n_h(\text{Cu})$ and $n_h(\text{O})$, which is supported by the theoretical works.¹⁸ Eventually, a doping level, $N_h = n_h(\text{Cu}) + n_h(\text{O})$ per one CuO_2 plane was evaluated for $n=1$ Tl2201, $n=2$ Y123O_{6+x}, $n=2$ Y1248, $n=2$ Bi2212 and $n=3$ Tl2223 compounds.^{7,17} Figure 5 indicates $K_{s,ab}(\text{RT})$ vs N_h plots for these compounds. As seen in the figure, $K_s(\text{RT})$ increases linearly with N_h , following

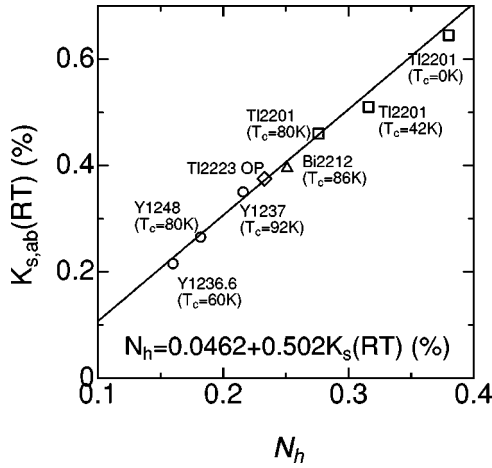


FIG. 5. The $K_{s,ab}(RT)$ at room temperature (RT) for the $n=1$ and $n=2$ compounds is plotted against its doping level N_h . N_h is a doping level in a layer $N_h = n_h(\text{Cu}) + n_h(\text{O})$ that are respective local hole densities at the planer Cu and O site. Here $n_h(\text{Cu})$ and $n_h(\text{O})$ were deduced from the respective nuclear quadrupole frequencies at the Cu and O site (Ref. 6). The solid line $N_h = 0.0462 + 0.502K_{s,ab}(RT)$ is a fit to the data.

an experimental relation of $N_h = 0.0462 + 0.502K_{s,ab}(RT)$. Note that the relation seen in Fig. 5 is valid irrespective of whether the CuO_2 plane is surrounded by the pyramidal or octahedral oxygen coordination.

Using this relation, we estimate $N_h(\text{OP})$ and $N_h(\text{IP})$ from the measured $K_{ab,s}(RT)$'s that are presented in Figs. 2 and 3. Thus estimated values are indicated in Table I. Here we have assumed that the hyperfine coupling constant is independent of IP or OP, which was actually confirmed in three-layered TI2223.⁷ Note that a total carrier content $\delta = (n-2)N_h(\text{IP}) + 2N_h(\text{OP})$ in a unit cell. In Fig. 6, $N_h(\text{OP})$, $N_h(\text{IP})$ and its difference $\Delta N_h = N_h(\text{OP}) - N_h(\text{IP})$ are plotted against an averaged hole content per a layer, $\delta_{av} = \delta/n$. In all the compounds, it is remarkable that $N_h(\text{OP})$ is larger than $N_h(\text{IP})$. Both $N_h(\text{OP})$ and $N_h(\text{IP})$ increase linearly as δ_{av} increases. ΔN_h increases with increasing δ , and also n such that $\Delta N_h = 0.025(n=3)$, $0.080(n=4)$, and $0.100(n=5)$, even if $\delta_{av} \sim 0.21$ is the same.

The present result on a systematic variation in $N_h(\text{OP})$ and $N_h(\text{IP})$ indicated in Fig. 6 is in good agreement with the theoretical prediction.^{19,20} For multilayered high- T_c cuprates, Di Stasio *et al.* argued a carrier distribution at each CuO_2 plane by using a sheet-charge model that assumes two-dimensional sheets of charge.¹⁹ Alternatively, Haines and Tallon modified the former model to a point-charge model, in which the sheet charge electrostatic term is replaced by a Madelung energy.²⁰ In both the models, a carrier distribution at each plane was calculated so as to minimize a total carrier energy expressed by a sum of band energy and electrostatic energy. Consequently, both the models showed that ΔN_h increases with increasing either δ or n , consistent with the present experiment. Considering an ionic configuration around the IP and OP, we may remark that the apical oxygen O^{2-} that is close to the OP lowers electrostatic energy for holes presenting at the OP than at the IP. As n increases, a

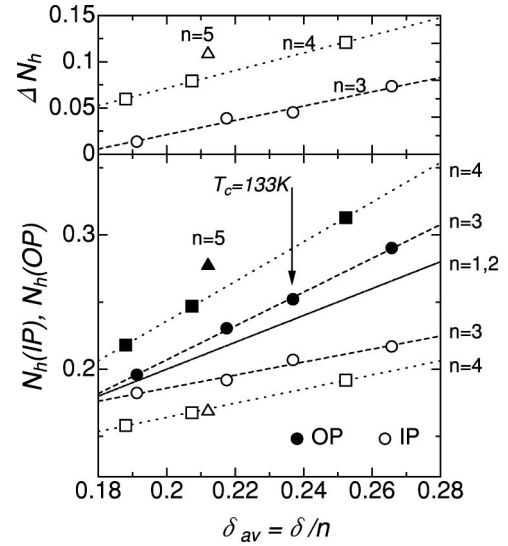


FIG. 6. Local doping levels at the OP and IP, $N_h(\text{OP})$, $N_h(\text{IP})$ and $\Delta N_h = N_h(\text{OP}) - N_h(\text{IP})$ are plotted against an average doping level $\delta_{av} = \delta/n$ for the $n=3, 4$, and 5 compounds [see [(a)–(h)] in Table I]. Here $\delta = (n-2)N_h(\text{IP}) + nN_h(\text{OP})$. Assuming a linear relation between $K_{s,ab}(RT)$ vs N_h in Fig. 5, $N_h(\text{OP})$ and $N_h(\text{IP})$ were estimated from the measured $K_{ab,s}(RT)$'s that are presented in Figs. 2 and 3. In all the compounds, note that $N_h(\text{OP})$ is larger than $N_h(\text{IP})$. Both $N_h(\text{OP})$ and $N_h(\text{IP})$ increase linearly with δ_{av} . ΔN_h increases as δ or n increases.

distance between the IP and the apical oxygen becomes larger, and then their difference of electrostatic energy is enhanced, making ΔN_h increase.²¹

As ΔN_h increases, it is evident that the IP and OP reveal the disparate SC and magnetic behaviors. For $\Delta N_h \leq \sim 0.07$, T_c , and T^* are uniquely determined as seen in Figs. 4(a–e), but for $\sim 0.07 \leq \Delta N_h$, T^* exists only for the IP and the SC gap at the OP begins to develop gradually below T_c and follows the BCS mean-field behavior of T dependence just below T_{c2} that is far below the bulk T_c . These results suggest that either a magnetic or an electronic interlayer coupling between the IP and OP for $n \geq 4$ becomes progressively weaker as ΔN_h increases. Once ΔN_h exceeds a critical value of ~ 0.07 , both the SC and magnetic properties are governed by the respective value of $N_h(\text{IP})$ and $N_h(\text{OP})$ that are underdoped and heavily overdoped, respectively.

Finally, we comment on a systematic variation in the T_c in the multilayered high- T_c cuprates. In most of high- T_c cuprates, it is known that T_c for the $n=1$ and $n=2$ compounds reaches a maximum value around an optimum $N_h(\text{optimum}) \sim 0.2$. For the $n=3, 4$, and 5 compounds, it is, however, hard that both the OP and IP are optimally doped because the electrostatic energy that is mainly generated by the apical oxygen is lower at the OP than at the IP. In the $n=3$ Hg1223, $T_c = 133$ K was reported to exhibit the highest T_c to date. In this compound, it is noteworthy that $N_h(\text{IP}) \sim 0.2$ is just optimized and $N_h(\text{OP}) \sim 0.25$ is comparable to $N_h(\text{optimum})$ as shown in Fig. 6. This suggests that the highest value in T_c to date is because the IP is optimally doped. This may be because the disorder at the IP is relatively small as seen in Fig. 1 and the plane is flatter than the

OP.¹³⁻¹⁵ It would be expected that its T_c increases further, reaching a record of high T_c , if $N_h(\text{OP})$ were reduced to ~ 0.2 . In the $n=4$ Hg1234 where the OP and IP reveal the similar SC and magnetic behaviors as seen in Fig. 4(e), its $T_c=123$ K is relatively higher than in Cu1234 [see Fig. 4(f)]. This is because a large difference in doping level between the IP and OP makes an interlayer coupling weaker in the latter. We suggest that a large ΔN_h reduces a bulk T_c . We propose that (i) an optimum hole doping at the IP and (ii) a decrease in ΔN_h are important factors for obtaining a further high T_c in multilayered cuprates.

III. CONCLUSION

In summary, we have studied through the ^{63}Cu Knight-shift measurements the magnetic and SC characteristics in the multilayered high- T_c cuprates, $\text{HgBa}_2\text{Ca}_{n-1}\text{Cu}_n\text{O}_{2n+2+y}$ and $\text{CuBa}_2\text{Ca}_{n-1}\text{Cu}_n\text{O}_{2n+4-y}$. Here the number of CuO_2 planes n ranges from $n=3$ to 5 and a total doping level δ varies from under- to over-doped region. Local doping levels $N_h(\text{IP})$ and $N_h(\text{OP})$ at the IP and OP have been separately extracted from the spin part in ^{63}Cu -Knight shift $K_s(\text{RT})$ at room temperature. The highest $T_c=133$ K to date in Hg1223 ($n=3$) was shown to arise because both the OP and IP are nearly optimally doped. As either δ or n increases, the OP is predominantly overdoped, whereas the IP remains underdoped. As a difference $\Delta N_h = N_h(\text{OP}) - N_h(\text{IP})$ increases,

the disparate magnetic and SC behaviors were found at the IP and OP such that the pseudogap behavior is seen alone at the IP, and a bulk SC transition does not set in simultaneously at the IP and OP. The energy gap at the OP seems to develop following the BCS mean-field type of T dependence below T_{c2} that is significantly lower than T_c . A T_c is not reduced even though these multilayered high- T_c compounds are heavily overdoped,¹ because the IP remains underdoped and keeps a high value of T_c , while the OP is heavily overdoped. This may be a microscopic origin for the lowest anisotropic SC characteristics ($\gamma \sim 1.4$) reported to date in Cu-based multilayered high- T_c compounds.² We propose that a homogeneous carrier distribution over all the CuO_2 planes is one of most important conditions to raise T_c , and to realize this, it may be efficient to reduce any difference in the electrostatic energy between the IP and OP. In this context, a replacement of the apical O^{-2} by F^{-1} is promising in reducing it as actually realized in the $\text{Ba}_2\text{Ca}_3\text{Cu}_4\text{O}_{10-x}\text{F}_x$ system.²² This study is now underway.

ACKNOWLEDGMENTS

This work was partly supported by the COE Research (10CE2004) in a Grant in Aid for Scientific Research from the Ministry of Education, Sports, Science and Culture of Japan. One of authors (Y.T.) was supported by JSPS.

*Core Research for Evolutional Science and Technology (CREST) of the Japan Science and Technology Corporation (JST)

¹T. Watanabe, H. Kashiwagi, S. Miyashita, N. Ichioka, K. Tokiwa, A. Iyo, Y. Tanaka, S.K. Agarwal, and H. Ihara, *J. Low Temp. Phys.* **117**, 753 (1999); T. Watanabe, S. Miyashita, N. Ichioka, K. Tokiwa, K. Tanaka, A. Iyo, Y. Tanaka, and H. Ihara, *Physica B* **284-288**, 1075 (2000).

²H. Ihara, K. Tokiwa, K. Tanaka, T. Tukamoto, T. Watanabe, H. Yamamoto, A. Iyo, M. Tokumoto, and M. Umeda, *Physica C* **283-287**, 957 (1997).

³S. Adachi, A. Tokiwa-Yamamoto, A. Fukuoka, R. Usami, T. Tatsuiki, Y. Moriwaki, and T. Tanabe, in *Studies of High Temperature Superconductors*, edited by A. V. Narlikar (Nova Science Publishers, New York, 1997), Vol.23 pp.:163-191.

⁴A. Trokiner, L.Le. Noc, J. Schneck, A.M. Pougnet, R. Mellet, J. Primot, H. Savary, Y.M. Gao, and S. Aubry, *Phys. Rev. B* **44**, 2426 (1991).

⁵B.W. Statt and L.M. Song, *Phys. Rev. B* **48**, 3536 (1993).

⁶G.-q. Zheng, Y. Kitaoka, K. Asayama, K. Hamada, H. Yamauchi, and S. Tanaka, *J. Phys. Soc. Jpn.* **64**, 3184 (1995).

⁷G.-q. Zheng, Y. Kitaoka, K. Asayama, K. Hamada, H. Yamauchi, and S. Tanaka, *Physica C* **260**, 197 (1996).

⁸K. Magishi, Y. Kitaoka, G.-q. Zheng, K. Asayama, K. Tokiwa, A. Iyo, and H. Ihara, *J. Phys. Soc. Jpn.* **64**, 4561 (1995).

⁹M.-H. Julien, P. Carreta, M. Horvatić, C. Berthier, Y. Berthier, P. Ségransan, A. Carrington, and D. Colson, *Phys. Rev. Lett.* **76**, 4238 (1996).

¹⁰Y. Piskunov, K.N. Mikhalev, Yu.I. Zhdanov, A.P. Geraschenko, S.V. Verkhovskii, K.A. Okulova, E.Yu. Medvedev, A.Yu.

Yakubovskii, L.D. Shustov, P.V. Bellot, and A. Trokiner, *Physica C* **300**, 225 (1998).

¹¹Y. Tokunaga, K. Ishida, Y. Kitaoka, K. Asayama, K. Tokiwa, A. Iyo, and H. Ihara, *Phys. Rev. B* **61**, 9707 (2000).

¹²H. Ihara, K. Tokiwa, H. Ozawa, M. Hirabayashi, A. Negishi, H. Matuhata, and Y.S. Song, *Jpn. J. Appl. Phys., Part 1* **33**, 503 (1994); *Jpn. J. Appl. Phys., Part 2* **33**, L300 (1994); *Physica C* **235-240**, 981 (1994); *Adv. Supercond.*, 1983 **VII**, 255 (1995).

¹³J. Akimoto, K. Tokiwa, A. Iyo, H. Ihara, H. Hayakawa, Y. Gotoh, and Y. Oosawa, *Physica C* **279**, 181 (1997).

¹⁴A. Bertinotti, D. Colson, J. Hammann, J-F. Marucco, D. Luzet, A. PinateL, and V. Viallet, *Physica C* **250**, 213 (1995).

¹⁵Y. Shimakawa, J.D. Jorgensen, D.G. Hinks, H. Shaked, R.L. Hitterman, F. Izumi, T. Kawashima, E. Takayama-Muromachi, and T. Kamiyama, *Phys. Rev. B* **50**, 16 008 (1994).

¹⁶H. Kotegawa, Y. Tokunaga, K. Ishida, Y. Kitaoka, H. Kito, A. Iyo, K. Tokiwa, T. Watanabe, and H. Ihara (unpublished).

¹⁷G.-q. Zheng, Y. Kitaoka, K. Ishida, and K. Asayama, *J. Phys. Soc. Jpn.* **64**, 2524 (1995).

¹⁸K. Hanzawa, F. Komatsu, and K. Yoshida, *J. Phys. Soc. Jpn.* **59**, 3345 (1990).

¹⁹M. Di Stasio, K.A. Müller, and L. Pietronero, *Phys. Rev. Lett.* **64**, 2827 (1990).

²⁰E.M. Haines and J.L. Tallon, *Phys. Rev. B* **45**, 3172 (1992).

²¹H. Kotegawa, Y. Tokunaga, K. Ishida, G.-q. Zheng, Y. Kitaoka, K. Asayama, H. Kito, A. Iyo, H. Ihara, K. Tanaka, K. Tokiwa, and T. Watanabe, *J. Phys. Chem. Solids* **62**, 171 (2001).

²²A. Iyo, K. Tokiwa, and H. Ihara (private communication).